Odd-even parity splittings and octupole correlations in neutron-rich Ba isotopes

Y. Fu, H. Wang, L.-J. Wang, and J. M. Yao

Phys. Rev. C **97**, 024338 — Published 27 February 2018

DOI: 10.1103/PhysRevC.97.024338

Odd-even parity splittings and octupole correlations in neutron-rich Ba isotopes

Y. Fu and H. Wang
School of Mechatronics Engineering, Guizhou Minzu University, Guiyang, 550001 China

L. -J. Wang* and J. M. Yao
Department of Physics and Astronomy, University of North Carolina, Chapel Hill, North Carolina 27516-3255, USA
(Dated: January 22, 2018)

The odd-even parity splittings in low-lying parity-doublet states of atomic nuclei with octupole correlations have usually been interpreted as rotational excitations on top of octupole vibration in the language of collective models. In this paper, we report a deep analysis of the odd-even parity splittings in the parity-doublet states of neutron-rich Ba isotopes around neutron number $N = 88$ within a full microscopic framework of beyond mean-field multi-reference covariant energy density functional theory. The dynamical correlations related to symmetry restoration and quadrupole-octupole shape fluctuation are taken into account with a generator coordinate method combined with parity, particle-number, and angular-momentum projections. We show that the behavior of odd-even parity splittings is governed by the interplay of rotation, quantum tunneling and shape evolution. Similar to ^{224}Ra, a picture of rotation-induced octupole shape stabilization in the positive-parity states is exhibited in the neutron-rich Ba isotopes.

PACS numbers: 21.10.-k, 21.10.Re, 21.60.Jz

I. INTRODUCTION

Atomic nuclei with neutron number or proton number around $34, 56, 88, 134$ are expected to have strong octupole correlations as there are single-particle partner states with orbital angular momentum difference $\Delta\ell = 3$ around Fermi surface [1–3]. These nuclei are characterized with the existence of low-lying parity-doublet states and enhanced electric octupole transition (E3) strengths. The typical example nuclei ^{144}Ba [4, 5] and ^{224}Ra [6] are suggested to have a stable reflection-asymmetric (or pear-like) shape in intrinsic frame. In contrast to the low-lying states with an alternating parity in reflection-asymmetric diatomic molecular systems, the negative-parity states $1^-, 3^-, 5^-, \ldots$ in octupole deformed nuclei are shifted up in energy with respect to positive-parity states $2^+, 4^+, 6^+, \ldots$ at low spin region. It seems that the negative- and positive-parity states form two different rotational bands. This peculiar feature, referred to as either *odd-even staggering* or *parity splitting*, indicates a possible existence of large quantum shape fluctuation in octupole shapes. On the other hand, the amplitude of parity splitting is gradually decreasing with the increase of spin and the two rotational bands merger into one. In other words, starting from a certain angular momentum I, a molecular-type band ordered in energy as $I^+, (I+1)^-, (I+2)^+, \ldots$, is exhibited. This phenomenon seems to be common in atomic nuclei with octupole correlations, even though their staggering amplitudes differ from each other in detail.

There are several attempts to explain the observed odd-even parity splittings based on different theoretical models. Nazarewicz *et al.* proposed to understand the parity splitting by studying the overlap of parity operator for the intrinsic state on which the two rotational bands are built, even though they did not provide a deep analysis of the parity splittings in their cranking Woods-Saxon-Bogoliubov method [7]. Jolos *et al.* proposed a picture of rotation-induced second-order phase transition from dynamical octupole to static octupole shapes based on a one-dimensional collective model with phenomenological spin-dependent potentials [8, 9]. Garrote *et al.* found that the octupole deformations of the negative- and positive-parity states in ^{144}Ba from a self-consistent cranked Hartree-Fock-Bogoliubov (HFB) calculation with parity projection are obviously different in low-spin region. As the spin increases up to a certain value, the octupole deformations become close to each other. These results indicate that the odd-even parity splittings are probably originated from the differently deformed intrinsic wave functions for the positive- and negative-parity states [10]. Minkov *et al.* proposed a collective model within which they ascribed the odd-even parity staggering to the interplay between the octupole shape oscillation mode and the stable quadrupole-octupole rotation mode [11]. Frauendorf interpreted the strong octupole correlations of rotational bands in the light actinides as the condensation of rotational-aligned octupole phonons [12]. He attributed the odd-even parity splittings to the discrete phonon energy and parity conservation. Recently, Yao *et al.* developed a beyond mean-field multi-reference covariant density functional theory (MR-CDFT) by implementing simultaneously particle number, parity, and angular momentum projections onto generator coordinate method (GCM) and applied this method to understand the spin-dependent parity splittings in ^{224}Ra [13]. It turns out that the attenuation of parity splitting amplitude with the increase of spin is related to the octupole shape stabilization of positive-

* ljwang@email.unc.edu

parity states, the shapes of which drift gradually toward those of negative-parity ones. This picture is close to, but containing more information from shape fluctuations than that by Garrote *et al.* [10] based on the cranking HFB calculation with parity projection.

The two questions to be asked naturally are 1) whether the picture exhibited in the low-spin parity-doublet states of ^{224}Ra also exists in octupole shaped nuclei of other mass region and 2) wether there is a direct connection between the spin-dependent staggering behaviors and nuclear shape evolution. The neutron-rich Ba isotopes provide good examples to analyze in deep the mechanisms for the spin-dependent parity splittings as the spectroscopic properties of their low-lying states with both positive and negative parities have been measured [4, 5, 14]. On the theoretical side, octupole correlations in the Ba isotopes have been demonstrated with either mean-field approaches [15–20], or a quadrupole-octupole collective Hamiltonian based on mean-field solutions [21, 22], or the interacting Boson model with Hamiltonian parameters fitted to the mean-field energy surface [23] or the most recent symmetry-conserved GCM [14, 24]. In the above theoretical studies, however, the mechanisms for the parity splittings are seldom discussed in detail.

The covariant density functional theory (CDFT) has achieved a great success in nuclear physics [25–28]. To go beyond mean-field approximation, projection techniques and GCM based on the mean-field solutions have been implemented into the CDFT. This beyond mean-field method is often called MR-CDFT, which has been applied to study the collective excitations of axially [29] and triaxially deformed nuclei [30–33]. Recently, this method has been extended to understand the spin-dependent parity splittings in the octupole deformed nucleus ^{224}Ra [13], the anharmonicity of multi-octupole-phonon excitations in ^{208}Pb [34], the molecular-like clustering structure in ^{20}Ne [35], the nuclear matrix elements of neutrinoless double beta decay [36–39], and the low-lying states of hypernuclei [40, 41].

In this paper, we present a comprehensive study of octupole correlations in Ba isotopes and perform a deep analysis of the mechanisms that are responsible for their spin-dependent parity splittings based on the MR-CDFT. We show that the staggering behaviors in excitation energies of odd-even spin states are governed by the interplay of rotation, quantum tunneling and shape evolution. All these effects can be taken into account simultaneously and full microscopically in the MR-CDFT. The paper is organized as follows. The framework of the MR-CDFT and numerical details are introduced in Sec. II. The properties of the low-lying states and the spin-dependent parity splittings in the neutron-rich Ba isotopes are discussed in Sec. III. A brief summary of this work is given in Sec. IV.

II. THE MODEL

In the MR-CDFT for nuclear quadrupole-octupole collective excitations, the wave functions $|\Psi^{J\pi}_{\alpha}\rangle$ of low-lying parity-doublet states are constructed as a linear combination of a set of quantum-number projected nonorthogonal mean-field states within the GCM framework,

$$|\Psi^{J\pi}_{\alpha}\rangle = \sum_{\kappa=\{K,\mathbf{q}\}} f^{J\pi\alpha}_{\kappa}\hat{P}^{\pi}|\Phi^{JKNZ}(\mathbf{q})\rangle, \tag{1}$$

where the $\hat{P}^{\pi}$ is the parity projection operator defined by the parity operator $\hat{P}$ as follows

$$\hat{P}^{\pi} = \frac{1}{2}(1+\pi\hat{P}). \tag{2}$$

The index $\alpha = 1, 2, \ldots$ in Eq. (1) labels different states for a given spin-parity J^{π}. The nonorthogonal wave function $|\Phi^{JKNZ}(\mathbf{q})\rangle$ is for an intrinsic state projected onto angular momentum J and particle numbers of neutrons (N) and protons (Z)

$$|\Phi^{JKNZ}(\mathbf{q})\rangle = \hat{P}^{J}_{MK}\hat{P}^{N}\hat{P}^{Z}|\mathbf{q}\rangle \tag{3}$$

where the expressions for the projection operators $\hat{P}^{G}$s ($G \equiv J, N, Z$) have been introduced in detail in textbook [42]. The generator coordinate $\mathbf{q}$ stands for the discritized deformation parameters $\{\beta_2, \beta_3\}$ of the reference states from deformation constrained selfconsistent mean-field calculation [43] based on a universal relativistic energy functional PC-PK1 [44]. The deformation parameters β_{λ} of quadrupole ($\lambda = 2$) and octupole ($\lambda = 3$) shapes are defined as

$$\beta_{\lambda} \equiv \frac{4\pi}{3AR^{\lambda}}\langle\mathbf{q}|r^{\lambda}Y_{\lambda 0}|\mathbf{q}\rangle, \quad R = 1.2A^{1/3}, \tag{4}$$

with A being mass number of the nucleus. The weight function $f^{J\pi\alpha}_{\kappa}$ and energy $E^{J\pi}_{\alpha}$ of each state J^{π} is determined with variational principle which leads to the Hill-Wheeler-Griffin equation,

$$\sum_{\kappa_b}\left[\mathscr{H}^{J\pi}_{\kappa_a,\kappa_b} - E^{J\pi}_{\alpha}\mathscr{N}^{J\pi}_{\kappa_a,\kappa_b}\right] f^{J\pi\alpha}_{\kappa_b} = 0 \tag{5}$$

where the Hamiltonian kernel $\mathscr{H}^{J\pi}_{\kappa_a,\kappa_b}$ and norm kernel $\mathscr{N}^{J\pi}_{\kappa_a,\kappa_b}$ are given by,

$$\mathscr{O}^{J\pi}_{\kappa_a,\kappa_b} = \langle\Phi^{JK_aNZ}(\mathbf{q_a})|\hat{O}\hat{P}^{\pi}|\Phi^{JK_bNZ}(\mathbf{q_b})\rangle \tag{6}$$

with the operator $\hat{O}$ representing $\hat{H}$ and 1, respectively.

The many-body wave functions $|\mathbf{q}\rangle$ for the whole atomic nucleus in intrinsic frame are generated from deformation constrained relativistic mean-field (RMF) plus BCS calculation, where the Dirac equation for single-particle wave functions is solved in a three dimensional isotropic harmonic-oscillator basis with 12 major shells. The oscillator frequency is given by $\hbar\omega_0 = 41A^{-1/3}$

(MeV). Axial and time-reversal symmetries are imposed to reduce the computational burden. In this case, the value of K in Eq. (1) is only zero and this index is dropped out subsequently. Two of the three Euler angles in the angular momentum projection can be carried out analytically. The numbers of mesh points in remaining one Euler angle for angular momentum projection and the gauge angle for particle number projection are chosen as 16 and 9, respectively. The Pfaffian formulas with the occupation probability truncated in canonical basis [45, 46] are implemented to calculate norm overlaps in the norm kernel. Details on the truncation of the model space have been introduced in Ref. [30]. The Hamiltonian kernel is calculated with the mixed-density prescription [47].The convenience of this choice regarding consistency with the mean field was discussed in Ref. [48] and the failure of other prescriptions presented in Ref. [49]. Though the prescription brings with it spurious divergences and "steps" in multi-reference energy density functional (EDF) calculation [50], it does not produce an unresolvable ambiguity when used together with the relativistic EDF that is a functional of densities and currents with integer powers. A set of about 40 reference states in the $(\beta_2, \beta_3 \geq 0)$ deformation plane is adopted in the GCM calculation. The configurations with $\beta_3 < 0$ are included automatically by using the parity operator. More details about the calculations with symmetry-conserved GCM are described in Refs. [31, 51, 52].

III. RESULTS AND DISCUSSIONS

Figure 1 displays the ratio $R_{J/2}$ of excitation energy of each state with angular momentum J to that of 2_1^+ state for neutron-rich Ba isotopes. It is seen that staggering behavior is exhibited in all the Ba isotopes that are concerned, even though the amplitude is somewhat different from each other. The staggering amplitude is overall decreasing with the increase of spin. These features are reasonably reproduced by the present configuration-mixing MR-CDFT calculation, except for ^{142}Ba. The quality of reproducing the patterns in $R_{J/2}$ provides us a confidence to analyze the underlying mechanisms responsible for the energy-staggering behavior in the parity-doublet states with the MR-CDFT. It is noted that the $R_{J/2}$ for ^{142}Ba as a function of angular momentum J deviates from data. As it will be discussed later, it is ascribed to the obviously overestimated excitation energy of the 2_1^+ state. A way to cure this deficiency is to adopt the intrinsic reference states optimized for each angular momentum J in the so-called projection-before-variation (PBV) scheme. In this case, the excitation energy of the 2_1^+ is expected to decrease as the rotational structure will be determined by the Thouless-Valatin moment of inertia, instead of the Yoccoz moment of inertia [42, 53]. As an approximation of the PBV, one may choose the cranked states without time-reversal invariance as the reference states in the GCM calculations [54]. Such kind of calculation is

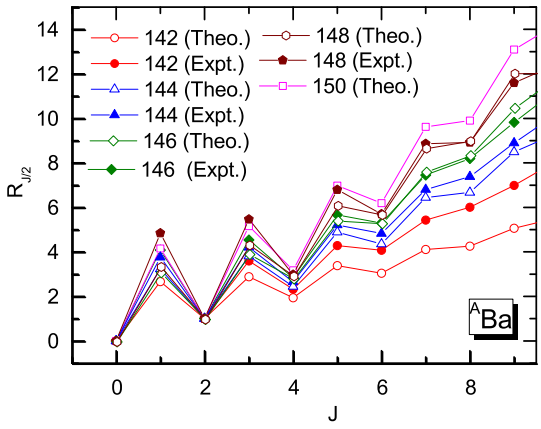

FIG. 1. (Color online) The ratio $R_{J/2}$ (defined as $E_x(J^\pi)/E_x(2_1^+)$) of the excitation energy of each J^π state to that of 2_1^+ state as a function of the angular momentum $J(\hbar)$. The filled symbols are for data, while the open symbols are for the results from the present configuration-mixing calculations.

beyond the scope of this work.

Supposing each spin-parity state J^π is built on a single configuration $|\mathbf{q}(\beta_2, \beta_3)\rangle$, one can derive the energy $E^{J\pi}(\mathbf{q})$ for the state J^π,

$$E^{J\pi}(\mathbf{q}) = \frac{\langle \hat{H} \rangle_{J\mathbf{q}} + \pi \langle \hat{H}\hat{P} \rangle_{J\mathbf{q}}}{\langle 1 \rangle_{J\mathbf{q}} + \pi \langle \hat{P} \rangle_{J\mathbf{q}}}, \tag{7}$$

where the overlap of the operator $\hat{O}$ is defined as $\langle \hat{O} \rangle_{J\mathbf{q}} \equiv \langle \Phi^{JNZ}(\mathbf{q}) | \hat{O} | \Phi^{JNZ}(\mathbf{q}) \rangle$. From the above expression for the energy of each spin-parity state, one can calculate the ratio $R_{J/2}$ for the spin-parity state J^π, which for odd J and negative parity has the following two limits

$$R_{J/2} \simeq \begin{cases} \dfrac{\langle \hat{H} \rangle_{J\mathbf{q}}}{\langle \hat{H} \rangle_{2\mathbf{q}}} \cdot \dfrac{\langle 1 \rangle_{2\mathbf{q}}}{\langle 1 \rangle_{J\mathbf{q}}} & , \ \langle \hat{P} \rangle_{J\mathbf{q}(\beta_3 \neq 0)} \to 0 \\ +\infty & , \ \langle \hat{P} \rangle_{J\mathbf{q}(\beta_3 \neq 0)} \to 1 \end{cases} \tag{8}$$

One notices that the overlap of parity operator for a reflection-asymmetric intrinsic state ($\beta_3 \neq 0$), $\langle \mathbf{q}(\beta_2, \beta_3) | \hat{P} | \mathbf{q}(\beta_2, \beta_3) \rangle = \langle \mathbf{q}(\beta_2, \beta_3) | \mathbf{q}(\beta_2, -\beta_3) \rangle$. This overlap is decreasing rapidly from one to zero with the increase of β_3, see Fig. 7 for ^{144}Ba or Ref. [13] for ^{224}Ra. From Eq. (8), one expects that the ratio $R_{J/2}$ with odd-J is a large number for the configuration with a small β_3 value. At a sufficient large value of β_3, the quantities $\langle \hat{P} \rangle_{J\mathbf{q}(\beta_3 \neq 0)}$ and $\langle H\hat{P} \rangle_{J\mathbf{q}(\beta_3 \neq 0)}$ approach to zero, in which case, the positive- and negative-parity states share a same energy expression, cf. Eq. (7). As a result, the negative-parity states merger into the band of positive-parity states and there is no staggering. Considering the fact that the overlap $\langle \hat{P} \rangle_{J\mathbf{q}}$ of a quantum-number (J, N, Z) projected state is usually much smaller than $\langle \mathbf{q} | \hat{P} | \mathbf{q} \rangle$, the speed of transition in between these

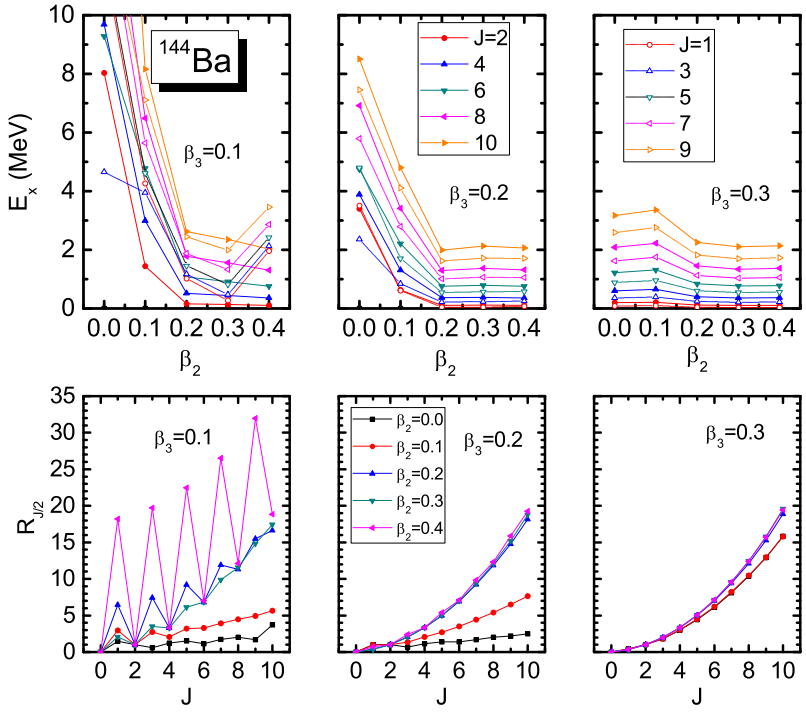

FIG. 2. (Color online) (Upper panels) The excitation energy of states projected onto particle number, angular momentum and parity based on an individual configuration for ^{144}Ba. (Lower panels) The ratio $R_{J/2}$ as a function of angular momentum $J(\hbar)$.

two limits is faster than that without the particle-number and angular momentum projections. The above analysis indicates that the overlap of parity operator $\langle\hat{P}\rangle_{J\mathbf{q}(\beta_3\neq\mathbf{0})}$, which reflects the penetrability of the barrier separating the two octupole minima at $\mathbf{q}(\pm\beta_\mathbf{3})$, affects the odd-even parity splittings and this effect is changing with the spin.

Taking ^{144}Ba as an example, we perform a detailed study on the excitation energy of parity-doublet states based on a set of differently shaped configurations with quadrupole deformation parameter $\beta_2 = 0.0, 0.1, 0.2, 0.3, 0.4$ and octupole deformation parameter $\beta_3 = 0.1, 0.2, 0.3$, respectively. Figure 2 displays the numerical results for the excitation energy and the ratio $R_{J/2}$ for each case. Obviously, one can see that the size of octupole deformation parameter plays a decisive role in the staggering behavior for the low-spin parity-doublet states. Specifically, one finds

- For $\beta_3 = 0.1$, the staggering amplitude increases roughly with the quadruple deformation parameter β_2 of the configuration. Moreover, spin-dependent staggering amplitude is exhibited even in the results of calculation based on a single configuration. This phenomenon can be understood from the spin-dependent overlap $\langle\hat{P}\rangle_{J\mathbf{q}}$.
- For $\beta_3 = 0.2$ or 0.3, the odd-even parity states are interleaving regardless of the value of quadruple deformation as the overlap $\langle\hat{P}\rangle_{J\mathbf{q}}$ is close to zero. There is no evident staggering.

The octupole deformation parameter of the predominant configuration is usually in between 0.1 and 0.2 and thus the energy spectra of these nuclei exhibit similar patterns to those displayed in the left-bottom panel ($\beta_2 = 0.1$ case) of Fig. 2. To the best of our knowledge, no one has found any single atomic nucleus that possesses interleaving odd-even parity states in their low-spin states as illustrated in the middle(right)-bottom panel of Fig. 2. Besides, it is interesting to notice that the 3^- state is predicted to be the first excited state for the configuration with $\beta_2 = 0$ and $\beta_3 = 0.1$, or 0.2. This is exactly the case that has been found in closed-shell nucleus like ^{208}Pb [34].

Let us move on to some realistic cases, the neutron-rich Ba isotopes around neutron number $N = 88$, in which there are mixings of differently quadrupole-octuple shaped configurations. Figure 3 displays mean-field energy surfaces of even-even Ba isotopes $^{140-154}$Ba in β_2-β_3 deformation plane. These energy surfaces are essentially the same as Fig.6 in Ref. [22]. Instead of constructing a collective Hamiltonian based the mean-field solutions, we carry out an exact GCM calculation in this work. The existence of octupole deformed minima in $^{144-150}$Ba is a consequence of strong octupole-octupole interactions between pairs of single-particle orbitals near the Fermi surface with orbital (ℓ) and total (j) angular momenta differing by $3\hbar$ around the Fermi level, i.e. the proton ($1h_{11/2}$, $2d_{5/2}$) and the neutron ($1i_{13/2}$, $2f_{7/2}$) in neutron-rich Ba

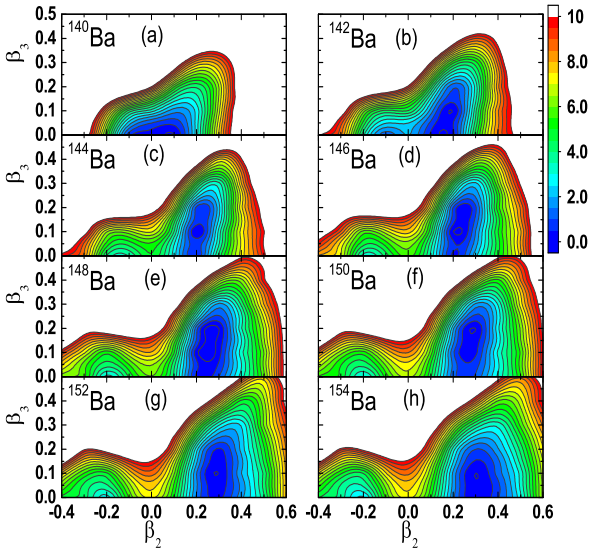

FIG. 3. (Color online) Mean-field energy surfaces (normalized to the energy minimum) for the neutron-rich Ba isotopes in β_2-β_3 deformation plane, where two neighboring lines are separated by 0.5 MeV.

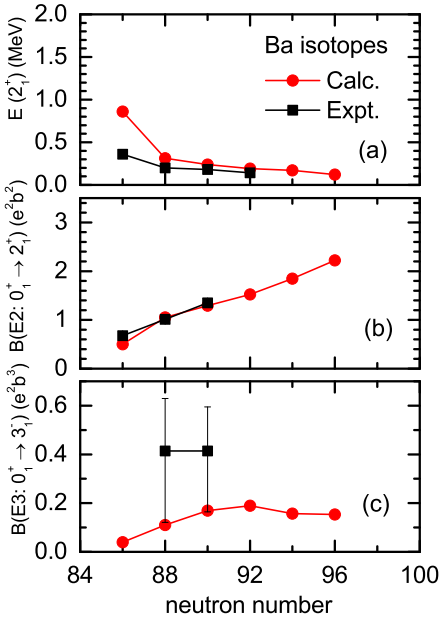

FIG. 4. (Color online) Systematics of the excitation energy of 2_1^+ state and the E2, E3 transition strengths in neutron-rich Ba isotopes around neutron number $N = 88$.

isotopes [15]. For ^{142,152,154}Ba, their energy surfaces are slightly softer in β_3 direction than those of $^{144-150}$Ba. Similar to what has been found in Th isotopes [55], the collectivity of both quadrupole and octupole types is developing as the neutron number increases from $N = 84$ to $N = 92$. The development of quadrupole and octupole

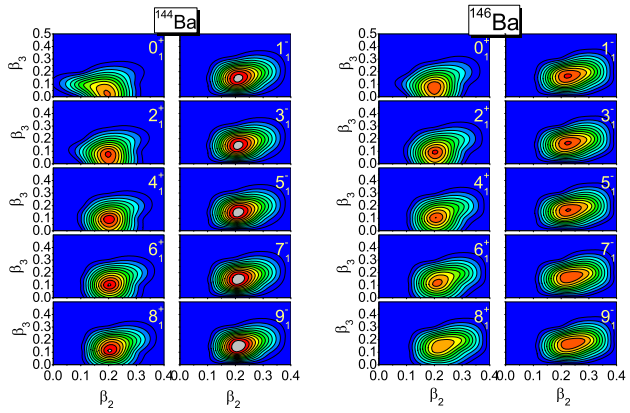

FIG. 5. (Color online) Evolution of collective wave functions for the parity-doublet states in the deformation β_2-β_3 plane for ^{144,146}Ba. See text for details.

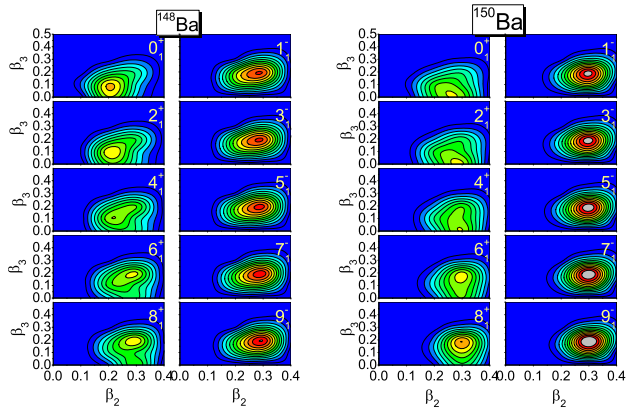

FIG. 6. (Color online) Same as Fig. 5, but for ^{148,150}Ba.

collectivity is demonstrated more clearly in the evolution of excitation energies of the 2_1^+ state and the $E2$, and $E3$ transition strengths, see Fig. 4. The corresponding data are reasonably reproduced except for the obvious overestimation of the excitation energy of the 2_1^+ state in ^{142}Ba. Together with the somewhat underestimation of the $E2$ transition strength between ground state and the 2_1^+ state, one may conclude that the quadrupole collectivity in ^{142}Ba is underestimated in the present calculation.

To understand the staggering behaviors in the low-lying parity-doublet states in neutron-rich Ba isotopes, c.f. Fig. 1, it is helpful to plot the distribution of their collective wave functions in β_2-β_3 plan. Figs. 5 and 6 display the collective wave functions $|g_\alpha^{J\pi}|^2$ for the low-lying parity-doublet states for ^{144,146,148,150}Ba, where the orthonormal collective wave function $g_\alpha^{J\pi}$ is constructed as $g_\alpha^{J\pi}(\mathbf{q}_a) = \sum_{\mathbf{q}_b} \left[\mathcal{N}^{J\pi}\right]^{1/2}_{\mathbf{q}_a,\mathbf{q}_b} f^{J\pi\alpha}_{\mathbf{q}_b}$. It is shown that the distribution of the collective wave function for the negative parity state is not evidently changed with the increase of spin, while that for the positive-parity states are changing gradually with spin and become close to that of

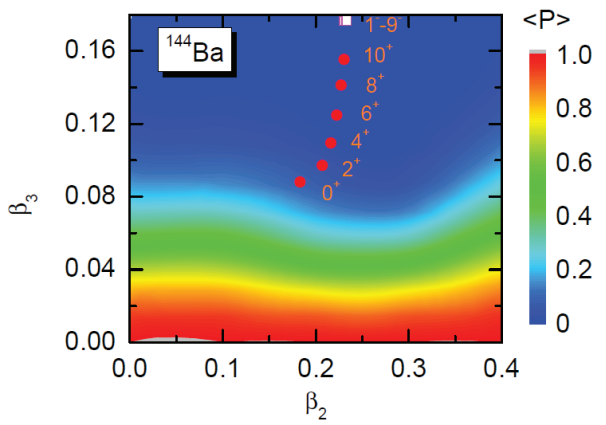

FIG. 7. (Color online) The distribution of the overlap $\langle \mathbf{q}|\hat{P}|\mathbf{q}\rangle$ of parity operator for each intrinsic state of ^{144}Ba in the β_2-β_3 plane. The average deformation $\langle\beta_\lambda\rangle \equiv \sum_q \beta_\lambda |g_\alpha^{J\pi}|^2$ with $\lambda = 2, 3$ and $J = 0, 1, \ldots, 10$ for the parity-doublet states in ^{144}Ba is indicated with filled circles ($\pi = +$) and open squares ($\pi = -$).

negative-parity state when the spin increases up to a certain value. In this evolution process, the octupole deformation of the predominant configuration for the positive-parity state is increasing and also becomes close to that for the negative parity state. It is shown more clearly in Fig. 7, where the average quadrupole-octupole deformation of each spin-parity state as a function of spin has been plotted. This picture is similar to that presented in the parity-doublet states of ^{224}Ra [13]. As discussed in Fig. 2, the $R_{J/2}$ is closely related to the quadrupole-octupole deformation of the configuration on which the energy spectrum is built. As the increase of spin up to $J = 10$, the average octupole deformation of even-spin and positive-parity states is increasing up to $\beta_3 \simeq 0.16$ and the odd-even staggering have the tendency to disappear, cf. the discussions on Fig. 2. Therefore, the shift of the predominant configuration in the positive-parity state with the increase of spin also affects the odd-even parity staggering behaviors in the neutron-rich Ba isotopes.

IV. SUMMARY

We have presented a symmetry-conserved beyond-mean-field study of low-lying parity-doublet states in neutron-rich Ba isotopes with the MR-CDFT, where the dynamical correlations related to restoration of broken symmetries and to fluctuations of quadrupole-octupole shapes have been taken into account with the exact generator coordinate method combined with particle-number, angular-momentum, and parity projections. Both the energy spectrum and the E2, E3 transitions are reasonably reproduced in a full microscopic way. Particular emphasis has been placed on the analysis of the odd-even parity splittings at the low-spin region. By carrying out a set of calculations based on a single configuration, we have demonstrated that the behavior of odd-even parity splittings is mainly governed by the quantity $\langle\hat{P}\rangle_{J\mathbf{q}}$, which is closely related to the configuration on which the energy spectrum is built. Moreover, the configuration-mixing calculations have shown that with the increase of spin, the shapes of the negative-parity states in the neutron-rich Ba isotopes are much more stable than those of positive-parity states, the predominant configuration of which is shifting from a weakly octupole deformed shape to that of negative-parity states. This picture is similar to that found in ^{224}Ra. It confirms the conjecture made in Ref. [13] that the rotation-induced octupole shape stabilization is a common phenomenon in some actinides and rare-earth nuclei. The above two analysis convince us that the spin-dependent parity splitting is governed not only by the octupole shape stabilization, but also by the interplay of rotation and quantum tunneling. We note that our present study is based on the static intrinsic states with time-reversal invariance. In other words, the reference states which server as the basis of GCM wave functions, are not allowed to change with angular momentum and only the mixing amplitudes vary with rotation. A more comprehensive way to study the evolution of nuclear shape with rotation requires the choice of cranked states as the reference states in the MR-CDFT calculation. Work along this direction is in progress.

ACKNOWLEDGMENTS

This work was supported by the National Natural Science Foundation of China under Grant Nos. 11575148, 11475140, 11305134 and the Scientific Discovery through Advanced Computing (SciDAC) program funded by US Department of Energy, Office of Science, Advanced Scientific Computing Research and Nuclear Physics, under Contract Nos. DE-SC0008641 and ER41896.

[1] I. Ahmad and P. A. Butler, Ann. Rev. Nucl. Part. Sci. 43, 71 (1993).
[2] P. Butler and W. Nazarewicz, Rev. Mod. Phys. 68, 349 (1996).
[3] P. A. Butler, J. Phys. G 43, 073002 (2016).
[4] W. R. Phillips, I. Ahmad, H. Emling, R. Holzmann, R. V. F. Janssens, and T.-L. Khoo, M. W. Drigert, Phys. Rev. Lett. 57, 3257 (1986).
[5] B. Bucher, S. Zhu, C. Y. Wu et al., Phys. Rev. Lett. 116, 112503 (2016).
[6] L. P. Gaffney et al., Nature 497, 199 (2013).

[7] W. Nazarewicz, P. Olanders, I. Ragnarsson, J. Dudek, G. A. Leander, Phys. Rev. Lett. 52, 1272 (1984).

[8] R. V. Jolos, and P. von Brentano, Phys. Rev. C92, 044318 (2015).

[9] R. V. Jolos and P. von Brentano, Phys. Rev. C 49, R2301(R) (1994); R. V. Jolos, P. von Brentano and J. Jolie, Phys. Rev. C 86, 024319 (2012).

[10] E. Garrote, J. L. Egido and L. M. Robledo, Phys. Lett. B410, 86 (1997); Phys. Rev. Lett. 80, 4398 (1998).

[11] N. Minkov et al, J. Phys. G: Nucl. Part. Phys. 32, 497 (2006).

[12] S. Frauendorf, Phys. Rev. C 77, 021304 (2008).

[13] J. M. Yao, E. F. Zhou, and Z. P. Li, Phys. Rev. C 92, 041304 (R) (2015).

[14] B. Bucher, S. Zhu, C. Y. Wu et al., Phys. Rev. Lett. 118, 152504 (2017).

[15] W. Zhang, Z. P. Li, S. Q. Zhang, Chin. Phys. C 34, 1094 (2010).

[16] L. M. Robledo, M. Baldo, P. Schuck, and X. Vinas, Phys. Rev. C 81, 034315 (2010).

[17] L. M. Robledo and G. F. Bertsch, Phys. Rev. C 84, 054302 (2011).

[18] H. L. Wang, J. Yang, M. L. Liu, and F. R. Xu, Phys. Rev. C 92, 024303 (2015).

[19] S. E. Agbemava, A. V. Afanasjev, and P. Ring, Phys. Rev. C 93, 044304 (2016).

[20] W. Zhang and Y. F. Niu, arXiv:1711.02234 [nucl-th].

[21] J. L. Egido and L. M. Robledo, Nucl. Phys. A518, 475 (1990).

[22] S. Y. Xia, H. Tao, Y. Lu, Z. P. Li, T. Niksic, and D. Vretenar, Phys. Rev. C 96, 054303 (2017).

[23] K. Nomura, D. Vretenar, T. Niksic, and B. N. Lu, Phys. Rev. C 89, 024312 (2014).

[24] R. N. Bernard, L. M. Robledo, and T. R. Rodriguez, Phys. Rev. C 93, 061302(R) (2016).

[25] P. Ring, Prog. Part. Nucl. Phys. 37, 193 (1996).

[26] D. Vretenar, A. V. Afanasjev, G. A. Lalazissis, P. Ring, Phys. Rep. 409, 101 (2005).

[27] J. Meng, H. Toki, S. G. Zhou, S. Q. Zhang, W. H. Long, L. S. Geng, Prog. Part. Nucl. Phys. 57, 470 (2006).

[28] J. Meng (ed), Relativistic Density Functional for Nuclear Structure (International Review of Nuclear Physics vol 10) (World Scientific), 2016.

[29] T. Nikšić, D. Vretenar, and P. Ring, Phys. Rev. C73, 034308 (2006); C74, 064309 (2006).

[30] J. M. Yao, J. Meng, P. Ring, and D. Pena Arteaga, Phys. Rev. C79, 044312 (2009).

[31] J. M. Yao, J. Meng, P. Ring and D. Vretenar, Phys. Rev. C81, 044311 (2010).

[32] J. M. Yao, H. Mei, H. Chen, J. Meng, P. Ring, D. Vretenar, Phys. Rev. C 83, 014308 (2011).

[33] J. M. Yao, K. Hagino, Z. P. Li, J. Meng, and P. Ring, Phys. Rev. C89, 054306 (2014).

[34] J. M. Yao, K Hagino, Phys. Rev. C 94, 011303 (R) (2016).

[35] E. F Zhou, J. M. Yao, Z. P. Li, J. Meng, P. Ring, Phys. Lett. B 753, 227 (2016).

[36] L. S. Song, J. M. Yao, P. Ring, J. Meng, Phys. Rev. C90, 054309 (2014); Phys. Rev. C95, 024305 (2017).

[37] J. M. Yao, L. S. Song, K. Hagino, P. Ring, J. Meng, Phys. Rev. C 91, 024316 (2015).

[38] J. M. Yao, J. Engel, Phys. Rev. C 94, 014306 (2016).

[39] J. Meng, L. S. Song, J. M. Yao, Int. Jour. Mod. Phys. E 26, 1740020 (2017).

[40] H. Mei, K. Hagino, J. M. Yao, T. Motoba, Phys. Rev. C90, 064302 (2014); 91, 064305 (2015); 93, 044307(2016); 96, 014308 (2017).

[41] H. Mei, K. Hagino, J. M. Yao, Phys. Rev. C 93, 011301 (R) (2016).

[42] P. Ring and P. Schuck, The Nuclear Many-Body Problem (Springer, Heidelberg, 1980).

[43] L. S. Geng, J. Meng, H. Toki, Chin. Phys. Lett. 24, 1865 (2007).

[44] P. W. Zhao, Z. P. Li, J. M. Yao, J. Meng, Phys. Rev. C 82, 054319 (2010).

[45] L. M. Robledo, Phys. Rev. C 79, 021302 (2009).

[46] G. F. Bertsch and L. M. Robledo, Phys. Rev. Lett. 108, 042505 (2012).

[47] P. Bonche, J. Dobaczewski, H. Flocard, P.-H. Heenen, J. Meyer, Nucl.Phys. A510, 466 (1990).

[48] L. M. Robledo, Int. J. Mod. Phys. E16, 337 (2007).

[49] L. M. Robledo, J. Phys. G: Nucl. Part. Phys. 37, 064020 (2010).

[50] D. Lacroix, T. Duguet, and M. Bender, Phys. Rev. C 79, 044318 (2009).

[51] M. Bender and P.-H. Heenen, Phys. Rev. C 78, 024309 (2008).

[52] T. R. Rodriguez and J. L. Egido, Phys. Rev. C 81, 064323 (2010).

[53] R. R. Rodriguez-Guzman, J. L. Egido, and L. M. Robledo, Phys. Rev. C 62, 054319 (2000).

[54] M. Borrajo, T. R. Rodriguez, and J. L. Egido, Phys. Lett. B 746, 341 (2015).

[55] Z. P. Li, B. Y. Song, J. M. Yao, D. Vretenar, J. Meng, Phys. Lett. B 726, 866 (2013).